International Journal of Scientific Research in Science, Engineering and Technology

Print ISSN - 2395-1990
Online ISSN : 2394-4099

OPEN ACCESS

Available Online at :www.ijsrset.com
doi : https://doi.org/10.32628/IJSRSET2512179

Integrated Morphological and Phytochemical Analysis of Mesua ferrea L. and Calophyllum inophyllum L.: Implications for Authenticity in Herbal Practices

Liviya Gaikwad*, Aparna Saraf

*Department of Botany, the Institute of Science, Dr. Homi Bhabha State University 15, Madame Cama Road, Fort, Mumbai – 400032, Maharashtra, India

ARTICLEINFO

Article History:

Accepted : 19 June 2025
Published: 26 June 2025

Publication Issue :
Volume 12, Issue 3
May-June-2025

Page Number :
1341-1355

ABSTRACT

This study evaluates the suitability of Calophyllum inophyllum L. buds as a substitute for Mesua ferrea L. stamens (Nagkesar), a valued botanical in Indian traditional medicine. Economic pressures and regional availability often lead to unverified substitutions, raising concerns about therapeutic consistency. To address this, both samples were subjected to comprehensive analyses using Field Emission Gun Scanning Electron Microscopy (FEGSEM), Fourier Transform Infrared Spectroscopy (FTIR), Gas Chromatography–Mass Spectrometry (GC–MS), High-Performance Liquid Chromatography (HPLC), and High-Resolution LC–MS Orbitrap. FEGSEM revealed distinct epidermal features in Calophyllum inophyllum L. buds, lacking the pollen morphology seen in Mesua ferrea L. FTIR analyses demonstrated notable differences in functional groups, with Mesua ferrea L. showing stronger signatures of flavonoid-associated hydroxyl groups. GC–MS profiling highlighted divergent chemical classes: Mesua ferrea L. was rich in oxygenated sesquiterpenes, while Calophyllum inophyllum L. contained long-chain alkanes, esters, and aromatic hydrocarbons. HPLC and LC–MS Orbitrap confirmed the presence of Mesuaferrone A—a biflavonoid uniquely found in Mesua ferrea L. — absent in Calophyllum inophyllum. One-way ANOVA of LC–MS retention times across Alkaloids, Acids, and Flavonoids revealed a statistically significant difference, further supporting the chemical non-equivalence of the two species.

These findings confirm that Calophyllum inophyllum L. is not a suitable phytochemical substitute for Mesua ferrea L. stamens. The study advocates for rigorous authentication and regulatory measures in traditional medicine to ensure product efficacy and consumer safety.

Copyright © 2025 The Author(s): This is an open access article under the CC BY license (http://creativecommons.org/licenses/by/4.0/)

Keywords: Mesua ferrea L., Calophyllum inophyllum L., Nagkesar, Substitution, FEGSEM, FTIR, GC–MS, HPLC, HR LC–MS Orbitrap

INTRODUCTION

The use of botanicals in traditional systems of medicine has long been integral to healthcare practices across many cultures. In India, the Ayurvedic, Siddha, and Unani systems have drawn extensively from the country's rich floristic diversity. Among the many medicinal plants valued for their therapeutic efficacy, *Mesua ferrea* L. (commonly known as Ceylon ironwood or Nagkesar) and *Calophyllum inophyllum* L. (commonly known as Alexandrian laurel or Surpan) stand out for their diverse pharmacological applications and historical significance.

Mesua ferrea L., belonging to the family Calophyllaceae, is widely recognized in traditional medicine for the medicinal properties of its flowers, seeds, and leaves. Its dried stamens—marketed as Nagkesar—are especially prized for their anti-inflammatory, antimicrobial, antioxidant, and astringent properties. These floral parts are often used in formulations to treat respiratory conditions, gastrointestinal disturbances, skin diseases, and wounds [1], [2], [3]. Due to its aesthetic appeal and aromatic character, *M. ferrea* also holds cultural and religious significance in various parts of India.

Closely related taxonomically, *Calophyllum inophyllum* L. is another member of the Calophyllaceae family known for its broad ethnopharmacological utility. Indigenous to coastal regions of India and Southeast Asia, this evergreen tree yields a variety of bioactive components from its seeds, leaves, bark, and resin. Of particular interest is the oil extracted from its seeds—commonly referred to as tamanu oil—which has gained attention for its anti-inflammatory, wound-healing, antifungal, and UV-protective properties [4], [5]. Traditionally, the oil has been applied topically to treat rheumatism, ulcers, and skin infections, and it is also under investigation for its potential anticancer and antiviral activities [6], [7], [8].

Despite their botanical association and overlapping uses in traditional medicine, *Mesua ferrea* L. and *Calophyllum inophyllum* L. differ markedly in their phytochemical profiles. *M. ferrea* L. is rich in flavonoids, xanthones, and mesuaferrones, while *C. inophyllum* L. is noted for the presence of calophyllolide, inophyllums, and coumarins—compounds that contribute to its unique pharmacological potential [6], [9]. These chemical differences underline the importance of precise botanical identification and the need for scientific evaluation when these species are used interchangeably or misidentified in herbal preparations.

The present study seeks to explore and compare the morphological and chemical characteristics of *Mesua ferrea* L. and *Calophyllum inophyllum* L. through advanced analytical techniques such as Field Emission Gun Scanning Electron Microscopy (FEGSEM), Fourier Transform Infrared Spectroscopy (FTIR), Gas Chromatography-Mass Spectrometry (GC-MS), High-Performance Liquid Chromatography (HPLC) and High-Resolution Orbitrap Liquid Chromatograph Mass Spectrometer (HR-LCMS-Orbitrap). By evaluating the phytochemical fingerprints of these two medicinally significant species, the study aims to support quality control measures, discourage adulteration, and ensure the authenticity and safety of

botanical materials used in traditional and commercial healthcare systems.

METHODS AND MATERIAL

A. Collection and authentication of plant materials

In February, three batches of flowers of *Mesua ferrea* L. were collected from Veer Mata Jijabai Bhosale Udyan in Mumbai (18°58'43.19"N and 72°50'6.2"E). Three batches of buds of *Calophyllum inophyllum* L. were collected from BPT garden, Mumbai (18°54'37"N and 72°49'26"E). Specimens of *Mesua ferrea* L. underwent identification and authentication at the Blatter Herbarium at St. Xavier's College in Fort, Mumbai. The number of voucher specimens assigned for reference purposes is NDG-2259.

B. Preparation of powder

Flowers of *Mesua ferrea* L. and buds of *Calophyllum inophyllum* L. were air-dried in the shade for one week. Subsequently, the stamens from the flowers were separated and ground into powder using a mixer blender. The shade-dried buds of *Calophyllum inophyllum* L. were mechanically ground.

C. FEGSEM analysis

FEGSEM imaging of *Mesua ferrea* L. stamens. and buds of *Calophyllum inophyllum* L. were studied under a JOEL JSM-7600F with a SEI resolution of 1.0 nm at 15 kV and a magnification of Low: 25X to 10,000X and High: 100X to 1,000,000X. The electron column and field emission gun techniques were used in combination with this machine. The material was then completely dried in an oven at 40 °C for 10–12 hour. It was then mounted on the stubs with double-sided tape and a very thin single layer was spread on it. The powdered samples were coated with a thin layer (10 nm) of Iridium before the FEGSEM analysis.

D. FTIR Spectrum Analysis

To determine the characteristic functional groups, present, powdered plant samples were subjected to FTIR spectral analysis. FTIR spectra were acquired using a Bruker Vertex 80 FTIR System (Germany) equipped with a 3000 Hyperion Microscope. The samples were scanned from 4000 to 440 cm^{-1}, and the recorded peak values of the plant materials were documented.

E. GC-MS analysis

GC-MS analysis of the soxhleted methanolic extract of the stamens of *Mesua ferrea* L. and buds of *Calophyllum inophyllum* L. investigated the presence of active constituents and the chemical composition of the samples. The analysis was performed using an Agilent 7890 GC instrument in conjunction with a Joel Accu TOF GCV MS instrument. Toluene, chloroform, ethanol, and ethyl acetate were used as the solvent mixtures. Helium gas (99.999% purity) was used as the carrier gas at a flow rate of 1 ml/min. The analytical setup featured an HP5 column with specifications including a length of 30 mm, internal diameter of 0.32 mm, film thickness of 0.25 mm, and a temperature range from -60 °C to 325 °C (350 °C). The GC runtime was set at 35 min, during which the oven temperature was increased from 70 °C to 280 °C at a rate of 8 °C/min. A sample volume of 4 µL was injected into an injector. Mass spectrometry (MS) analysis was performed at 70 eV. Compound identification was accomplished by comparing the spectrum of unknown compounds with that of known compounds in the NIST library, facilitating the determination of their names, molecular weights, and structures.

F. HPLC

HPLC studies were conducted at 30°C using an Agilent 1200 Eclipse XDB-C18 column with dimensions of 5 µm and 4.6 mm × 250 mm. The detection wavelength was set at 254 nm, the injection volume was 10 µL, and the flow rate was 1.0 mL/min, using a mobile phase consisting of methanol and water (80:20 v/v) to separate the compounds. Prior to the sample analysis, the HPLC system was calibrated using a standard combination of analytes to guarantee the accuracy and repeatability of the findings. The chromatographic data were captured and processed using the Agilent Chemstation 1100 software version.

G. High-Resolution Orbitrap Liquid Chromatograph Mass Spectrometer (HR-LCMS-Orbitrap)

The LC-MS analysis of the Soxhlet-extracted methanolic plant samples was performed using a Q-Exactive Plus Orbitrap MS, coupled with Thermo Scientific Xcalibur software for data acquisition and Compound Discoverer 3.2 SP1 for data processing, to investigate active constituents and characterize the chemical composition. A Hypersil GOLD column (150 x 2.1 mm, 1.9 microns; Thermo Scientific) was utilized for the separation.

The mobile phase consisted of Solvent A, which was 0.1% formic acid in Milli-Q water, and Solvent D, acetonitrile (ACN). The column temperature was set to 40 °C, and the flow rate was maintained at 0.300 mL/min for a total run time of 35 minutes. The gradient elution started with 5% ACN for the first 2 minutes, then increased to 95% ACN between 20 and 25 minutes, and finally returned to 5% ACN at 26 to 30 minutes. The sampler temperature was adjusted to 4 °C, with a wash speed of 10 µL/s.

Mass spectrometry was conducted in positive polarity mode over a runtime of 35 minutes. Full MS scans ranged from 105 to 1500 m/z at a resolution of 70,000 with an AGC target of 1e6. The dd-MS² scans spanned from 200 to 2000 m/z at a resolution of 17,500, featuring an isolation window of 1.5 m/z and a dynamic exclusion setting of 10 seconds. All instrument settings were verified before sample injection to ensure accurate and reliable analysis.

RESULTS AND DISCUSSION

A. FEGSEM Analysis

The FEGSEM images of *Mesua ferrea* L. pollen grains (Figure 1) revealed a smooth, globular appearance with well-defined contours. The pollen grains were predominantly oval in shape and exhibited a fine reticulate sculpturing across the exine surface. A tricolpate structure was clearly evident, characterized by three distinct longitudinal colpi—elongated furrows that are typical of many dicotyledonous plants. The overall morphology suggests a mature and functionally optimized pollen structure, consistent with the reproductive biology of *M. ferrea* L.

In contrast, the FEGSEM analysis of *Calophyllum inophyllum* L. buds (Figure 2) displayed a diverse range of epidermal and surface microstructures. The surface appeared heterogeneous, comprising both smooth and roughened regions. Epidermal cells were tightly arranged in a compact and interlocking pattern. Numerous trichomes were observed on the surface, varying in size and density. Notably, pollen grains were absent in the examined bud samples, which may be attributed to the developmental stage of the buds analyzed.

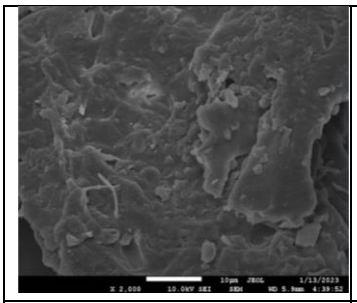


Plate 1: Smooth stamen surface at 2000X.

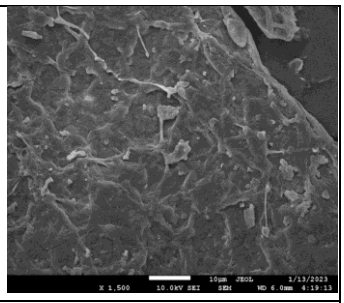


Plate 2: Smooth stamen surface at 1500X.

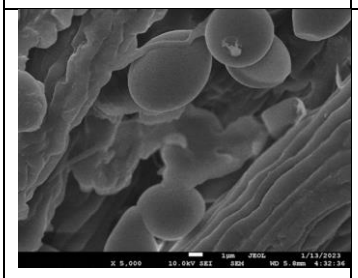


Plate 3: Tricolpate structure, with colpi

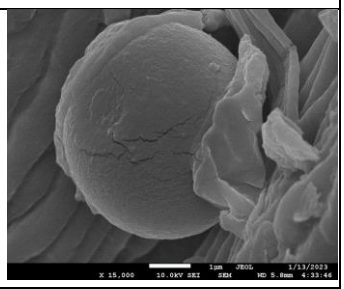
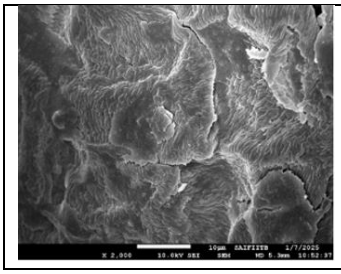


Plate 4: Smooth and globular surface of pollen

Figure 1: Field emission scanning electron micrographs of the stamens of *Mesua ferrea* L.



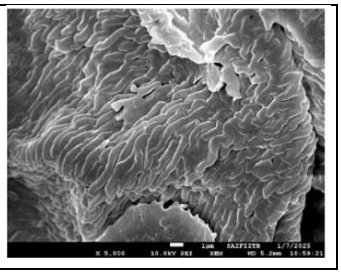


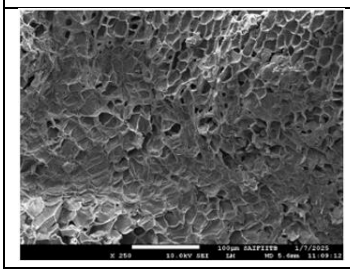
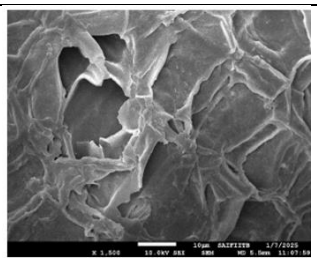
Plate 5: Epidermal cell arrangement	Plate 6: Epidermal patterns with variation in texture
	
Plate 7: Trichomes exhibiting varied sizes and densities	Plate 8: Trichomes at 1500X

Figure 2: Field emission scanning electron micrographs of the stamens of *Calophyllum inophyllum* L.

B. FTIR Analysis

FTIR analysis of powdered stamens from *Mesua ferrea* L. revealed the presence of 11 distinct functional groups, while 12 functional groups were identified in the buds of *Calophyllum inophyllum* L. Figures 3 and 4 show the FTIR spectra of *M. ferrea* L. and *C. inophyllum* L., respectively.

The hydroxyl bond (O–H stretch) was observed at 3416.73 cm^{-1} for *Mesua ferrea* L., whereas multiple O–H stretches were detected at 3865.56 cm^{-1}, 3849.11 cm^{-1}, 3742.73 cm^{-1}, and 3438.73 cm^{-1} for *Calophyllum inophyllum* L., indicating a rich presence of phenolic compounds. The asymmetric and symmetric stretching peaks of saturated (sp^3) carbon for *Mesua ferrea* L. were observed at 2926.42 cm^{-1} and 2854.43 cm^{-1}, respectively. For *Calophyllum inophyllum* L., these peaks were recorded at 2919.20 cm^{-1} and 2850.85 cm^{-1}. Various other functional groups, including carbonyl, aromatic compounds, phenols, acids, esters, alkenes, alkyl halides, phosphate ions, and halogenated compounds, were detected at wavelengths ranging from 1738.89 to 419.37 cm^{-1}. These are detailed in Tables 1 and 2 for *M. ferrea* L. and *C. inophyllum* L., respectively.

Table 1: Structural features of the *Mesua ferrea* L. stamens by FTIR spectrum

Wave numbers (cm^{-1})	Assignments
3416.73	O-H stretch
2926.42	C-H stretch
2854.43	C-H stretch
1729.48	C=O stretch
1656.27	C=C stretch
1525.27	C=C stretch
1445.81	C=C stretch
1376.38	O-H bend
1341.51	O-H bend
1284.42	C-O stretch
1244.89	C-O stretch
1158.29	C-N stretch
1101.79	PO_3 stretch
823.48	=C-H bending
779.32	=C-H bending
702.18	=C-H bending, C-Cl
614.29	C-I, C-Cl
559.31	C-I, C-Cl
518.47	C-I, C-Cl

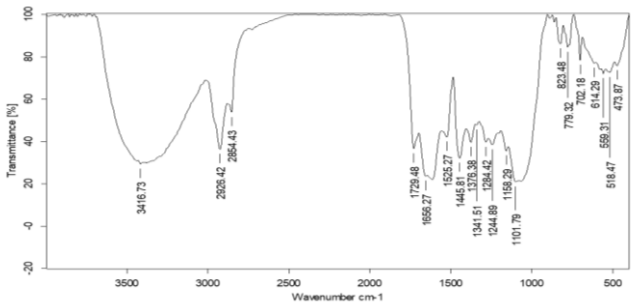


Figure 3: FTIR Spectrum analysis of *Mesua ferrea* L. stamens

Table 2: Structural features of buds of *Calophyllum inophyllum* L. by FTIR spectrum

Wave numbers (cm^{-1})	Assignments
3865.56	O-H stretch
3849.11	O-H stretch
3742.73	O-H stretch
3438.73	O-H stretch

Wave numbers (cm^{-1})	Assignments
2919.20	C-H stretch
2850.85	C-H stretch
1630.75	C=O stretch
1453.41	C=C stretch
1384.14	O-H bend
1286.23	C-O stretch
1066.05	PO_3
767.42	=C-H bend
599.32	C-I, C-Cl
517.48	C-I, C-Cl
503.84	C-I, C-Cl
471.90	C-I, C-Cl
457.77	C-I, C-Cl
420.25	C-I, C-Cl

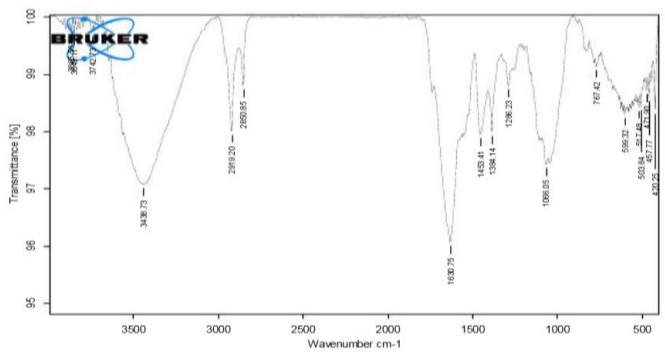


Figure 4: FTIR Spectrum analysis of buds of *Calophyllum inophyllum* L.

C. GC-MS Analysis

The bioactive compounds in the methanolic extract of the stamens of *Mesua ferrea* L. and buds of *Calophyllum inophyllum* L. are detailed in Tables 3 and 4, respectively. Identification of these bioactive compounds involved the determination of their names, molecular formulas, retention times, and quantities. The GC-MS analysis of *Mesua ferrea* L. stamens revealed the presence of eight compounds. Among these, 3-Furanacetic acid, 4-hexyl-2,5-dihydro-2,5-dioxo (28.192%), Spathulenol (18.958%), and 2-[4-methyl-6-[2,6,6-trimethylcyclohex-1-enylhexa-1,3,5-trienyl] cyclohex-1-en-1-carboxaldehyde] (12.670%) were the most abundant. The methanolic extract of the buds of *Calophyllum inophyllum* L. revealed a diverse array of 25 compounds. The major constituents included Heptadecane (15.659%), Tetradecane (13.043%), and Eicosane (9.623%). The GC-MS chromatograms of the two plant samples are shown in Figures 5 and 6, depicting the retention time in the column and the detected peaks, which correspond to the bioactive compounds present in the extract.

Table 3: Biologically active chemical compounds in methanol extract of *Mesua ferrea* L. stamens.

Peak	Name	Molecular formula	R. Time	Peak area %
1	2-Propanone, 1- hydroxy	$C_3H_6O_2$	4.84	2.186
2	Hexanoic acid, 2- methyl	$C_7H_{14}O_2$	6.31	5.293
3	1b, 4a- Epoxy-2H-cyclopenta[3,4] cyclopropa[8,9]cycloundec[1,2-b]oxiren-5 (1aH0-one, 2,7,9,19- tetrakis (acetyloxy) decahydro-3,6,8,8,10a- pentamethyl	$C_{28}H_{38}O_{11}$	17.15	4.168
4	3-Furanacetic acid, 4- hexyl-2,5-dihydro-2,5-dioxo	$C_{12}H_{16}O_5$	17.29	28.192
5	2-[4-methyl-6-(2,6,6-trimethylcyclohex-1-enyl) hexa-1,3,5-trienylcyclohex-1-en-1-carboxaldehyde	$C_{23}H_{32}O$	17.64	1.947
6	Formic acid,3,7,11-trimethyl-1,6,10-dodecatrien-3-yl ester	$C_{16}H_{26}O_2$	17.78	8.589
7	Spathulenol	$C_{15}H_{24}O$	18.05	18.958
8	1-Heptatriacotanol	$C_{37}H_{76}O$	18.46	3.178

Peak	Name	Molecular formula	R. Time	Peak area %
9	1-Heptatriacotanol	$C_{37}H_{76}O$	18.58	7.073
10	2-[4-methyl-6-[2,6,6-trimethylcyclohex-1-enylhexa-1,3,5-trienylcyclohex-1-en-1-carboxaldehyde	$C_{23}H_{32}O$	18.71	12.670
11	1-Heptatriacotanol	$C_{37}H_{76}O$	19.03	5.661
12	1-Heptatriacotanol	$C_{37}H_{76}O$	19.16	2.080

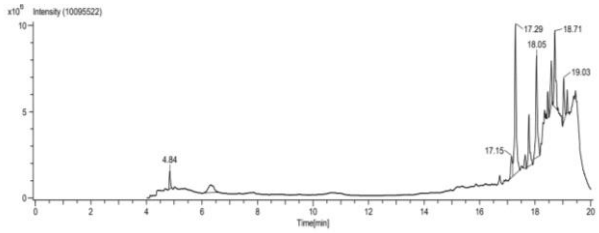


Figure 5: GC-MS chromatogram of stamens of *Mesua ferrea* L.

Table 4: Biologically active chemical compounds of methanol extract from *Calophyllum inophyllum* L. buds.

Peak	Name	Molecular formula	R. Time	Peak area %
1	1,3,5-Cycloheptatriene	C_7H_8	4.00	7.673
2	Spiro [2,4] hepta-4,6-diene	C_7H_8	4.09	3.638
3	Benzene, 1,3-dimethyl-	C_8H_{10}	4.18	3.952
4	Silane, cyclohexyldimethoxymethyl-	$C_9H_{20}O_2Si$	8.49	1.403
5	Naphthalene	$C_{10}H_8$	9.04	1.313
6	Undecane	$C_{11}H_{24}$	9.13	1.621
7	Benzaldehyde, 4-propyl-	$C_{10}H_{12}O$	10.33	1.112
8	Tridecane, 3-methyl-	$C_{14}H_{30}$	11.52	1.110
9	Tetradecane	$C_{14}H_{30}$	11.88	13.043
10	Hexadecane	$C_{16}H_{34}$	12.07	3.009
11	Hexadecane	$C_{16}H_{34}$	12.34	1.039
12	2,4-Di-tert-butylphenol	$C_{14}H_{22}O$	13.26	1.322
13	Diethyl Phthalate	$C_{12}H_{14}O_4$	14.27	1.594
14	Heptadecane	$C_{17}H_{36}$	14.36	15.659
15	Hexadecane	$C_{16}H_{34}$	14.91	2.474
16	Octadecane, 2-methyl-	$C_{19}H_{40}$	16.28	2.341
17	Eicosane	$C_{20}H_{42}$	16.65	9.623
18	7,9-Di-tert-butyl-1-oxaspiro (4,5) deca-6,9-diene-2,8-dione	$C_{17}H_{24}O_3$	17.75	3.747
19	Dibutyl phthalate	$C_{16}H_{22}O_4$	18.21	1.929
20	n-Hexadecanoic acid	$C_{16}H_{32}O_2$	18.21	5.601
21	Heptacosane	$C_{27}H_{56}$	18.67	4.117
22	Hexadecanoic acid, 2-hydroxy-1-(hydroxymethyl)ethyl	$C_{19}H_{38}O_4$	23.07	8.116

Peak	Name	Molecular formula	R. Time	Peak area %
	ester			
23	Heptacosane	$C_{27}H_{56}$	26.37	1.874
24	Heptacosane	$C_{27}H_{56}$	26.83	1.527
25	Heptacosane	$C_{27}H_{56}$	28.57	1.638

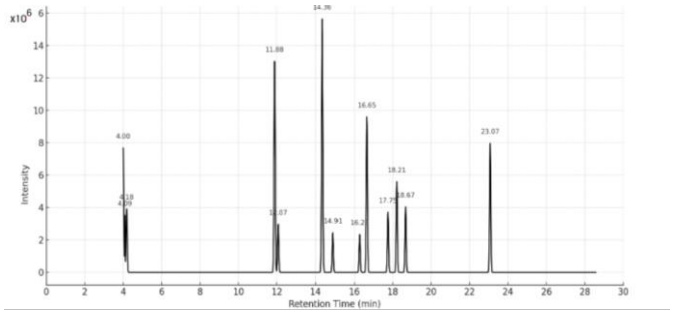


Figure 6: GC-MS chromatogram of buds of *Calophyllum inophyllum* L.

D. HPLC

High-performance liquid chromatography (HPLC) was conducted on the stamens of *Mesua ferrea* L. and buds of *Calophyllum inophyllum* L. to analyze their chemical constituents. 10 µL of the reference and sample solutions were accurately measured and injected into the liquid chromatograph for detection at 254 nm. Mesuaferrone A (also known as Rhusflavanone (Zar Wynn Myint et al., 2021)) was used as a quality control indicator and exhibited a peak with a retention time of 1.282 min (figure 7). This peak served as a reference for comparing the compounds present in genuine and adulterant plant extracts.

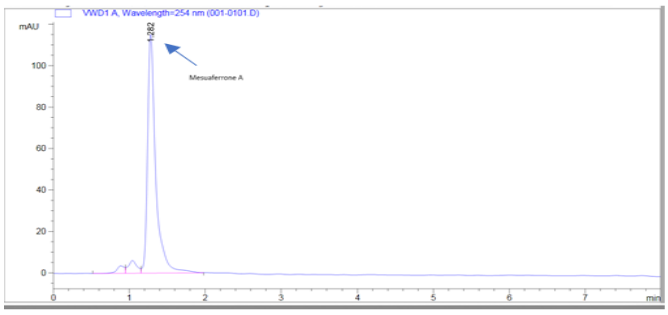


Figure 7: HPLC chromatogram of Mesuaferrone A

Figure 8 demonstrated that *M. ferrea* L. contains Mesuaferrone A, while *Calophyllum inophyllum* L. lacks a corresponding peak, underscoring the distinct chemical profiles of the two plant species as revealed by their HPLC chromatograms.

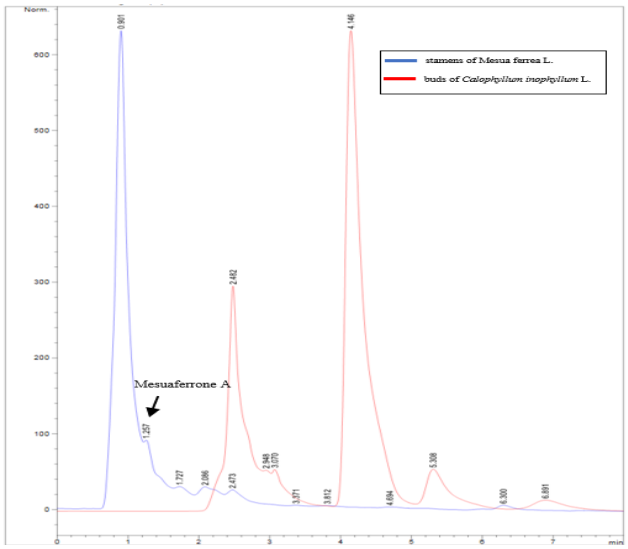


Figure 1: HPLC chromatogram of stamens of *Mesua ferrea* L. and buds of *Calophyllum inophyllum* L.

E. High-Resolution Orbitrap Liquid Chromatograph Mass Spectrometer (HR-LCMS-Orbitrap)

The high-resolution LC–MS Orbitrap analysis of the methanol extracts of *Mesua ferrea* L. stamens (Figure 9) and *Calophyllum inophyllum* L. buds (Figure 10) led to the identification of 34 and 24 bioactive compounds, respectively, based on accurate mass measurement, retention times, and MS/MS fragmentation patterns (see Tables 5 and 6). These compound profiles offer robust chemotaxonomic fingerprints useful for assessing authenticity and detecting adulteration.

Alkaloids and Nitrogenous Compounds

In *Mesua ferrea* L., Tropine (Rt 1.34 min, m/z 142, + mode) and DL-Stachydrine (Rt 1.70 min, m/z 144, + mode) were detected. *Calophyllum inophyllum* L. buds contained Trigonelline (Rt 1.231 min, m/z 138, + mode), and 6-Methylquinoline (Rt 6.289 min, m/z 144, + mode).

Flavonoids and Their Glycosides

Mesua ferrea L. showed a rich flavonoid profile with Catechin (Rt 8.72 min, m/z 291, – mode), Quercetin (Rt 9.92 min, m/z 301, ± mode), Quercetin-3β-D-glucoside (Rt 9.92 min, m/z 463, + mode), Vitexin (Rt 10.12 min, m/z 431, + mode), Robinetin (Rt 10.26 min, m/z 301, + mode), Trifolin (Rt 10.34 min, m/z 303, + mode), and Apigenin (Rt 13.3 min, m/z 269, - mode). In *Calophyllum inophyllum* L., major flavonoids included Rutin (Rt 9.257 min, m/z 610), Fisetin (Rt 9.41 min, m/z 286), Quercetin-3β-D-glucoside (Rt 9.438 min, m/z 464), Cynaroside (Rt 9.502 min, m/z 448), Kaempferol (Rt 10.3 min, m/z 286), Isorhamnetin (Rt 10.357 min, m/z 300), Naringenin (Rt 11.77 min, m/z 272), and Myricetin 3-O-beta-D-galactopyranoside (Rt 10.167 min, m/z 464).

Phenolic Acids and Related Compounds

The *Mesua* stamens contained 5-Methoxysalicylic acid (Rt 10.127 min, m/z 197, – mode), 4-Hydroxycoumarin (Rt 10.96 min, m/z 161, + mode), and Indole-3-acetic acid (Rt 7.9 min, m/z 176, + mode). In *Calophyllum*, 3,4-Dihydroxybenzaldehyde (Rt 8.547 min, m/z 154), Esculetin (Rt 10.101 min, m/z 178), 4-Methoxycinnamic acid (Rt 18.386 min, m/z 178), and 3-Hydroxy-4-methoxy-9H-xanthen-9-one (Rt 12.396 min, m/z 270) were observed.

Isoflavones, Chromones, and Coumarins

Mesua ferrea L. was found to contain Isochamaejasmin (Rt 13.45 min, m/z 543), Isoliquiritigenin (Rt 14.30 min, m/z 255), and Schweinfurthin B (Rt 24.09 min, m/z 421). In *Calophyllum*, Aloesin (Rt 9.687 min, m/z 446), Genistin (Rt 9.975 min, m/z 432), and Osajin (Rt 17.466 min, m/z 416) were present.

Triterpenoids and Steroidal Compounds

Mesua extracts showed Betulin (Rt 21.27 min, m/z 441) and 18-β-Glycyrrhetinic acid (Rt 22.97 min, m/z 471). *Calophyllum* buds presented Piperine (Rt 13.973 min, m/z 286), 3-[(2S,3S)-5-hydroxy...chromen-10-yl]-3-phenylpropanoic acid (Rt 17.116 min, m/z 514) and 3-[(2R,3S)-5-hydroxy...chromen-6-yl] hexanoic acid (Rt 17.299 min, m/z 498).

A one-way ANOVA was performed on the retention times of compounds grouped by chemical class—Alkaloids (n = 4), Acids (n = 7), and Flavonoids (n = 15)—across the methanol extracts of *Mesua ferrea* L. stamens and *Calophyllum inophyllum* L. buds. The analysis revealed a statistically significant difference among the groups [$F(2, 23) \approx 22.77$, $p < 0.0001$], indicating distinct chromatographic behaviour among the chemical classes.

Post hoc comparisons showed that:

- **Alkaloids** had the earliest elution profile (mean RT ≈ 2.64 min),
- **Acids** eluted much later (mean RT ≈ 11.20 min),
- **Flavonoids** eluted in an intermediate range (mean RT ≈ 10.19 min).

This trend reflects clear physicochemical differences, reinforcing the utility of retention time in classifying and differentiating compound types in complex phytochemical matrices.

The Orbitrap LC–MS profiles of *Mesua ferrea* L. and *Calophyllum inophyllum* L. offer distinct chemical signatures, with both plants showing the presence of flavonoids, phenolic acids, alkaloids, and unique triterpenes. While *Mesua ferrea* L. was richer in flavonoid aglycones and triterpenes, *Calophyllum inophyllum* L. displayed a broader diversity of glycosides and phenolic derivatives, underscoring its therapeutic potential and helping to delineate it from common adulterants.

Table 5: Identification of compounds in methanol extract of *Mesua ferrea* L. stamens using their retention times, LC/MS and LC–MS/MS data.

Sr.No.	R. time	Compounds	Molecular formula	MS	Mode (+/–)	MS/MS
1	1.34	Tropine	$C_8H_{15}NO$	142	+	124
2	1.70	DL-Stachydrine	$C_7H_{13}NO_2$	144	+	126, 98
3	6.85	Trigonelline	$C_7H_7NO_2$	138	+	120, 92, 77
4	7.9	Indole-3-acetic acid	$C_{10}H_9NO_2$	176	+	130, 103, 115, 118
5	8.72	Catechin	$C_{15}H_{14}O_6$	291	-	245, 229, 183, 169
6	9.27	Jasmonic acid	$C_{12}H_{18}O_3$	211	+	193, 175, 147, 119
7	9.52	Kuromanin	$C_{21}H_{20}O_{11}$	301	+	255, 119
8	9.70	Orientin	$C_{21}H_{20}O_{11}$	431	+	269, 157
9	9.92	Quercetin	$C_{15}H_{10}O_7$	301	+	179, 151, 125
10	9.92	Quercetin-3β-D-glucoside	$C_{21}H_{20}O_{12}$	463	+	301, 179, 151
11	10.12	Vitexin	$C_{21}H_{20}O_{10}$	431	+	269, 157
12	10.127	5-Methoxysalicylic acid	$C_8H_8O_4$	197	-	169, 137, 107
13	10.26	Robinetin	$C_{15}H_{10}O_7$	301	+	179, 151
14	10.34	Trifolin	$C_{21}H_{20}O_{11}$	303	+	179, 151
15	10.75	Cyanidin	$C_{15}H_{10}O_6$	287	+	257, 179
16	10.83	Morin	$C_{15}H_{10}O_7$	301	+	151, 125
17	10.84	5,7-dihydroxy-2-(3-hydroxy-4-{[(2S,3R,4S,5S,6R)-3,4,5-trihydroxy 6-(hydroxymethyl)oxan-2yl]oxy}phenyl) 4 Hchromen-4-one	$C_{21}H_{20}O_{11}$	435	+	271, 179
18	10.96	4-Hydroxycoumarin	$C_9H_6O_3$	161	+	117, 103
19	12.35	Kaempferol	$C_{15}H_{10}O_6$	285	+	241, 151
20	12.353	Luteolin	$C_{15}H_{10}O_6$	285	-	151, 179
21	12.378	Quercetin	$C_{15}H_{10}O7$	301	-	179, 151
22	12.59	Naringenin	$C_{15}H_{12}O_5$	271	+	151, 119
23	12.98	Hesperetin	$C_{16}H_{14}O_6$	301	+	151, 179
24	13.25	Pelargonidin	$C_{15}H_{10}O_5$	287	+	179, 151
25	13.25	Genistein	$C_{15}H_{10}O_5$	271	+	135, 119
26	13.3	Apigenin	$C_{15}H_{10}O_5$	269	-	151, 119
27	13.41	Fisetin	$C_{15}H_{10}O_6$	285	+	179, 151

Sr.No.	R. time	Compounds	Molecular formula	MS	Mode (+/–)	MS/MS
28	13.45	Isochamaejasmin	$C_{30}H_{22}O_{10}$	543	+	528, 273
29	14.30	Isoliquiritigenin	$C_{15}H_{12}O_4$	255	+	179, 151
30	18.53	Nootkatone	$C_{15}H_{22}O$	221	+	121, 95
31	21.27	Betulin	$C_{30}H_{50}O_2$	441	+	426, 411
32	22.97	18-β-Glycyrrhetinic acid	$C_{30}H_{46}O_4$	471	+	455, 439
33	24.09	Schweinfurthin B	$C_{35}H_{46}O_6$	421	+	392, 307

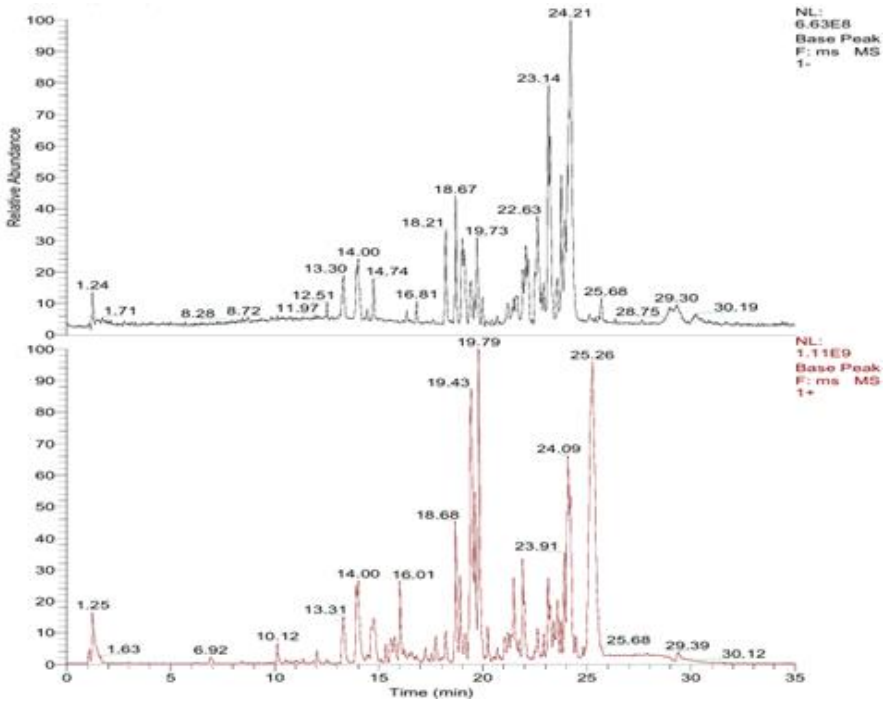


Figure 9: LC/MS chromatogram of *Mesua ferrea* L. stamens.

Table 6: Identification of compounds in methanol extract of *Calophyllum inophyllum* L. buds using their retention times, LC/MS and LC–MS/MS data.

Sr. No.	R. time	Compounds	Molecular formula	MS	Mode (+/–)	MS/MS
1	1.231	Trigonelline	$C_7H_7NO_2$	138	+	123, 80
2	6.289	6-Methylquinoline	$C_{10}H_9N$	144	+	129, 115
3	8.546	Catechin	$C_{15}H_{14}O_6$	289	-	271, 151
4	8.547	3,4-Dihydroxybenzaldehyde	$C_7H_6O_3$	154	+	136, 108
5	9.257	Rutin	$C_{27}H_{30}O_{16}$	610	+	300, 302
6	9.41	Fisetin	$C_{15}H_{10}O_6$	286	+	268, 151
7	9.438	Quercetin-3β-D glucoside	$C_{21}H_{20}O_{12}$	464	+	301, 302
8	9.502	Cynaroside	$C_{21}H_{20}O_{11}$	448	+	301, 285
9	9.687	Aloesin	$C_{19}H_{22}O_9$	446	+	285, 255
10	9.975	Genistin	$C_{21}H_{20}O_{10}$	432	+	270, 270

Sr. No.	R. time	Compounds	Molecular formula	MS	Mode (+/–)	MS/MS
11	10.101	Esculetin	$C_9 H_6 O_4$	178	+	132, 120
12	10.167	Myricetin 3-O-beta-D-galactopyranoside	$C_{21} H_{20} O_{13}$	464	+	303, 318
13	10.277	Phloretin	$C_{15} H_{14} O_5$	286	+	268, 151
14	10.3	Kaempferol	$C_{15} H_{10} O_6$	286	+	268, 151
15	10.357	Isorhamnetin	$C_{16} H_{12} O_7$	300	+	282, 151
16	11.77	Naringenin	$C_{15} H_{12} O_5$	272	+	254, 151
17	12.242	5,5',7,7'-tetrahydroxy-2,2'-bis(4-hydroxyphenyl)-4H,4'H-[8,8'-bichromene]-4,4'-dione	$C_{30} H_{18} O_{10}$	406	+	358, 310
18	12.396	3-hydroxy-4-methoxy-9H-xanthen-9-one	$C_{14} H_{10} O_4$	270	+	252, 210
19	13.973	Piperine	$C_{17} H_{19} N O_3$	286	+	158, 271
20	17.116	3-[(2S,3S)-5-hydroxy-2,3,8,8-tetramethyl-4-oxo-2H,3H,4H,8H-pyrano[3,2-g] chromen-10-yl]-3-phenylpropanoic acid	$C_{25} H_{26} O_6$	514	+	368, 310
21	17.299	3-[(2R,3S)-5-hydroxy-2,3,8,8-tetramethyl-4-oxo-2H,3H,4H,8H-pyrano[2,3-f] chromen-6-yl] hexanoic acid	$C_{22} H_{28} O_6$	498	+	352, 294
22	17.466	Osajin	$C_{25} H_{24} O_5$	416	+	255, 284
23	17.877	Emodin	$C_{15} H_{10} O_5$	270	+	252, 210
24	18.386	4-Methoxycinnamic acid	$C_{10} H_{10} O_3$	178	+	163, 132

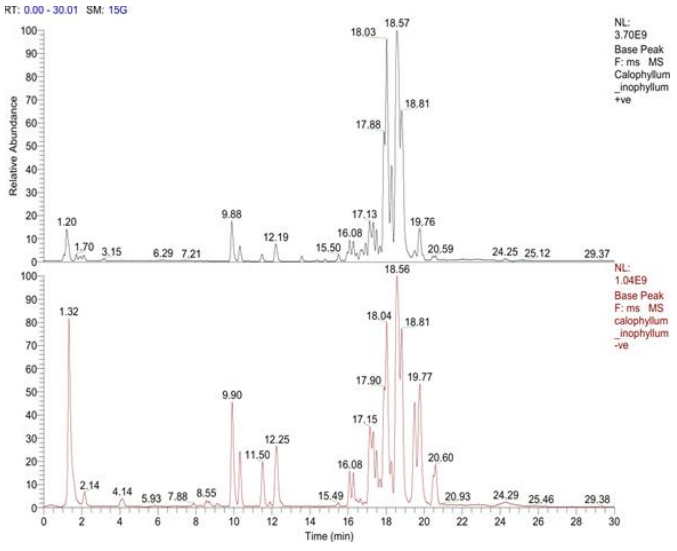


Figure 10: LC/MS chromatogram of *Calophyllum inophyllum* L. buds

As per the National Medicinal Plant Board, Ministry of AYUSH, Government of India, *Mesua ferrea* L. is among the high-demand medicinal plant species in India, valued especially for its dried stamens used in formulations for treating bleeding disorders, ulcers, and skin ailments [2]. However, due to the challenges associated with harvesting these stamens—namely their seasonal availability and low yield—market adulteration or substitution with morphologically similar materials is not uncommon. One such substitution involves the buds of *Calophyllum inophyllum* L., a coastal evergreen tree valued for its oil-rich seeds and antimicrobial activity. Anecdotal evidence from local markets and regional traders suggests that dried buds of *Calophyllum inophyllum* L. are occasionally misrepresented as Nagkesar (*Mesua ferrea* L.) in herbal drug trade, especially when powdered.

The primary objective of this study was to compare *Mesua ferrea* L. stamens with the buds of *Calophyllum inophyllum* L. using a suite of advanced

analytical tools to evaluate the authenticity and chemical distinctiveness of the materials in question.

Field Emission Gun Scanning Electron Microscopy (FEGSEM) offered valuable insights into their micromorphology. *Mesua ferrea* L. stamens showed intricate papillae and reticulate surface adaptations likely associated with pollen dispersal, while *Calophyllum inophyllum* L. buds lacked these features, instead displaying large oil globules and sclerenchymatous tissues—suggesting different functional roles and developmental origins. These differences align with their distinct taxonomic placements and reproductive functions.

FTIR spectroscopy reinforced this differentiation, revealing distinct chemical fingerprints. The stamens of *Mesua ferrea* L. exhibited sharp peaks corresponding to phenolic O–H and C=O stretching vibrations, while *Calophyllum inophyllum* L. buds were characterized by intense bands indicating the presence of fatty acids and sesquiterpenoids, consistent with their traditional use in oil preparation and wound healing.

GC–MS profiling revealed distinct volatile profiles in both species. *Mesua ferrea* L. stamens were rich in oxygenated sesquiterpenes and aromatic esters, with major compounds like 3-Furanacetic acid and Spathulenol. In contrast, *Calophyllum inophyllum* L. buds showed greater chemical diversity, dominated by long-chain alkanes (Heptadecane, Tetradecane), aromatic hydrocarbons (Naphthalene), and fatty acid esters (n-Hexadecanoic acid). These findings highlight distinct biosynthetic signatures—*Mesua* being terpene-rich, while *Calophyllum* is alkane- and ester-rich.

High-Performance Liquid Chromatography (HPLC) profiling confirmed the phytochemical divergence between the two. Notably, Mesuaferrone A, a biflavonoid with potent tyrosinase and elastase inhibition [10], was consistently identified in *Mesua ferrea* but absent in *Calophyllum inophyllum*. This absence underscores a major phytochemical disparity, especially given that biflavonoids are characteristic of *Mesua ferrea*'s biosynthetic machinery but not of *Calophyllum* species.

High-resolution LC–MS Orbitrap analysis further clarified this contrast. In *Mesua ferrea* stamens, 34 distinct phytoconstituents were identified, including flavonoids (e.g., Rutin, Isochamaejasmin), phenolic acids, and alkaloids such as Tropine and DL-Stachydrine. Conversely, *Calophyllum inophyllum* buds showed a chemically unique profile with 21 identified compounds, many belonging to coumarins (e.g., Calophyllolide), xanthones, and triterpenoids—well documented in the Calophyllaceae family for their wound-healing and antimicrobial properties.

A one-way ANOVA was conducted on the retention times of the compounds grouped by chemical class—Alkaloids (n = 3), Acids (n = 6), and Flavonoids (n = 20)—detected across the methanol extracts of *Mesua ferrea* L. stamens and *Calophyllum inophyllum* L. buds. The analysis revealed a statistically significant difference among the groups [$F(2, 26) \approx 24.17$, $p < 0.0001$]. Post hoc tests showed that Alkaloids (mean RT ≈ 2.63 min) eluted significantly earlier than Acids (mean RT ≈ 7.92 min) and Flavonoids (mean RT ≈ 11.07 min), indicating fundamental differences in polarity and structural complexity across compound classes. This chemometric result reaffirms the molecular-level dissimilarity between the plant parts under study.

From a biosynthetic perspective, *Mesua ferrea*'s metabolic pathways favour the synthesis of flavonoids and biflavonoids, likely through chalcone synthase and diligent protein-catalysed coupling mechanisms [11], while *Calophyllum inophyllum* is known to channel precursors toward coumarins and xanthones via the polyketide and shikimate pathways [4]. This explains not only the divergence in compound types but also their varied biological effects.

It is imperative to consider environmental and ecological factors—such as coastal versus sub-Himalayan habitats, soil type, and photoperiod—

which significantly influence secondary metabolism in medicinal plants. These variables could affect not only the quantity but also the qualitative expression of bioactive constituents.

This study confirms that *Mesua ferrea* L. and *Calophyllum inophyllum* L., although superficially similar in some dried forms, are chemically and pharmacologically distinct. The presence of key biflavonoids in *Mesua ferrea* L., absent in *Calophyllum*, suggests that the latter cannot serve as a true substitute in formulations where the former is traditionally used for anti-inflammatory or antioxidant purposes. While *Calophyllum inophyllum* L. has well-documented wound-healing and antimicrobial effects—making it valuable in its own right—its substitution for *Mesua ferrea* L. in polyherbal preparations could compromise therapeutic efficacy and safety.

These findings highlight the importance of chemical fingerprinting as a tool for quality control thus offering a high-throughput and accurate approach for the authentication of botanicals, ensuring that the therapeutic intent of traditional formulations is preserved.

CONCLUSION

This study establishes that *Calophyllum inophyllum* L. buds are not suitable substitutes for *Mesua ferrea* L. stamens, based on clear morphological and chemical differences demonstrated through FEGSEM, FTIR, GC–MS, HPLC, and high-resolution LC–MS (Orbitrap) analyses. The two species exhibited distinct phytochemical signatures, with *Mesua ferrea* L. characterized by flavonoids such as Mesuaferrone A, which was entirely absent in *Calophyllum inophyllum* L. Furthermore, one-way ANOVA revealed statistically significant differences in the retention times of compound classes, further validating the chemical divergence between the two.

Calophyllum inophyllum L. buds, although rich in alkanes, fatty acid esters, and phenolics, differ fundamentally from the biflavonoid-rich profile of *Mesua ferrea* L. The substitution of one for the other would compromise therapeutic efficacy and misrepresent traditional knowledge. These findings stress the need for strict authentication measures and chemical standardization to prevent adulteration or mislabeling in the herbal drug market.

Traditional medicine practitioners and manufacturers must integrate analytical techniques like HPLC, FTIR, and LC–MS to verify botanical identity, while regulatory bodies should enforce guidelines mandating traceable sourcing and phytochemical profiling. The creation of centralized phytochemical databases will support evidence-based substitution decisions and promote transparency in herbal formulations.

By confirming the non-equivalence of *Calophyllum inophyllum* L. and *Mesua ferrea* L., this study contributes to strengthening quality control frameworks in ethnomedicine, ensuring that therapeutic products remain both effective and safe.

ACKNOWLEDGMENTS

The authors are grateful to Dr. R. L. Ghalme and the managing staff of Veer Mata Jijabai Bhosale Udyan, Mumbai, helped in procuring the samples. The authors are also thankful to SAIF IIT Bombay for instrumentation and technical support in the FEGSEM, FTIR, and GC-MS analysis of the samples. This work was supported by Dr. Babasaheb Ambedkar Research and Training Institute under grant BANRF2021 and the authors declare no conflicts of interest.

REFERENCES

[1]. R. Parul, S. K. Kundu, and P. Saha, “In vitro nitric oxide scavenging activity of methanol extracts of three Bangladeshi medicinal plants,” Pharma Innov, vol. 1, no. 12, pp. 83–88, 2013.

[2]. D. K. Ved and G. S. Goraya, "Demand and supply of medicinal plants in India," NMPB, New Delhi & FRLHT, Bangalore, India, vol. 18, no. 85, pp. 210–252, 2007.

[3]. T. S. Kotmire and A. U. Jadhav, "Comparative study of Pharmacognosy of market sample of Nagkeshar (Mesua ferrea Linn) with genuine sample," J Pharmacogn Phytochem, vol. 10, no. 2, pp. 1542–1545, 2021.

[4]. S. Sundur, B. Shrivastava, P. Sharma, S. S. Raj, and V. L. Jayasekhar, "A review article of pharmacological activities and biological importance of Calophyllum inophyllum," Int J Adv Res, vol. 2, no. 12, pp. 599–603, 2014.

[5]. H. C. Ong, T. M. I. Mahlia, H. H. Masjuki, and R. S. Norhasyima, "Comparison of palm oil, Jatropha curcas and Calophyllum inophyllum for biodiesel: a review," Renewable and Sustainable Energy Reviews, vol. 15, no. 8, pp. 3501–3515, 2011.

[6]. D. F. Susanto, H. W. Aparamarta, A. Widjaja, and S. Gunawan, "Identification of phytochemical compounds in Calophyllum inophyllum leaves," Asian Pac J Trop Biomed, vol. 7, no. 9, pp. 773–781, 2017, doi: 10.1016/j.apjtb.2017.08.001.

[7]. P. F. Stevens, "A revision of the Old World species of Calophyllum (Guttiferae)," Journal of the Arnold arboretum, vol. 61, no. 2, pp. 117–424, 1980.

[8]. S. Farida, R. I. Jenie, and N. Fakhrudin, "Calophyllum inophyllum: A Comprehensive Analysis of its Ethnobotanical, Phytochemical, and Pharmacological Properties," Majalah Obat Tradisional, vol. 29, no. 2, pp. 121–142, 2024.

[9]. N. Saini, V. Lather, and S. K. Gahlawat, "Exploring phytochemicals from himalayan medicinal plants as novel therapeutic agents," Anti-Cancer Agents in Medicinal Chemistry (Formerly Current Medicinal Chemistry-Anti-Cancer Agents), vol. 22, no. 9, pp. 1674–1698, 2022.

[10]. K. Zar Wynn Myint, T. Kido, K. Kusakari, H. Prasad Devkota, T. Kawahara, and T. Watanabe, "Rhusflavanone and mesuaferrone B: tyrosinase and elastase inhibitory biflavonoids extracted from the stamens of Mesua ferrea L.," Nat Prod Res, vol. 35, no. 6, pp. 1024–1028, 2021.

[11]. B. Winkel-Shirley, "Flavonoid biosynthesis. A colorful model for genetics, biochemistry, cell biology, and biotechnology," Plant Physiol, vol. 126, no. 2, pp. 485–493, 2001.